Model Order-Reduction of RC(L) Interconnect including Variational Analysis†

Ying Liu, Lawrence T. Pileggi and Andrzej J. Strojwas
Department of Electrical and Computer Engineering
Carnegie Mellon University
5000 Forbes Avenue, Pittsburgh, PA 15213
yingl@ece.cmu.edu, pileggi@ece.cmu.edu, ajs@ece.cmu.edu

ABSTRACT

As interconnect feature sizes continue to scale to smaller dimensions, long interconnect can dominate the IC timing performance, but the interconnect parameter variations make it difficult to predict these dominant delay extremes. This paper presents a model order-reduction technique for RLC interconnect circuits that includes variational analysis to capture manufacturing variations. Matrix perturbation theory is combined with dominant-pole-analysis and Krylov-subspace-analysis methods to produce reduced-order models with direct inclusion of statistically independent manufacturing variations. The accuracy of the resulting variational reduced-order models is demonstrated on several industrial examples.

1. INTRODUCTION

Due to the complicated physical and chemical processes involved in the manufacturing of today's microelectronic devices, there will always be discrepancies between the conceptual design and the manufactured product. Typical examples of these *manufacturing variations* are fluctuations in critical dimensions (CD) and inter-level dielectric (ILD) thicknesses. These manufacturing variations are random in nature, and significant effort is continually aimed at minimizing the process variability. These fluctuations cannot be eliminated, however, and have been continuously increasing in relative magnitude as new generations of the deep submicron (DSM) technologies are introduced.

Typically, the effect of these process variations are captured by a set of worst-case SPICE model parameters. The impact on circuit performance is then estimated via multiple circuit simulations to explore the "worst-case corners". However, for RLC interconnect analysis these "parameter corners" can no longer guarantee the worst/best-case delay calculation accuracy due to the way in which resistance and capacitance inversely vary as a function of actual width and thickness. Moreover, the delay variations of the interconnect are now of the size and correlation complexity that the true critical path can go undetected when process variations are not considered. In addition, the delay variations due to interconnect parameter fluctuations produce clock skews that are well beyond the acceptable limits for today's high performance microprocessors. A Monte Carlo method or one of its design-of-experiment (DOE) variations can produce the required delay accuracy, but these approaches are prohibitively expensive due to the large number of simulations required.

One possible approach to avoid the expensive Monte Carlo technique is the interval analysis method[5]. In the interval method proposed in [5], the Rubinstein-Penfield model[12], which is essentially min/max bounds about the Elmore delay, is used to represent the RC interconnect delay. For DSM technologies the Elmore delay accuracy is insufficient due to the increasing magnitude of the interconnect series resistance that is not fully captured in this model. The higher order macromodels obtain via moment matching[10] or Krylov subspace methods[3][9][13] can produce the required accuracy; however, interval methods are not readily incorporated into these algorithms.

In this paper, we present a model order-reduction technique for interconnect that includes variational analysis. The technique is based on matrix perturbation expansion theory and extensions to existing interconnect model order-reduction methods. The new technique uses a few model order-reduction procedures to generate a complete variational reduced-order model in which the true manufacturing variations are explicitly incorporated. The variational reduced-order model can be then used for further delay and waveform calculation purposes.

2. BACKGROUND

2.1. Properties of manufacturing variations and key assumptions

As has been shown in many research reports, the true causes of manufacturing variations are very complicated[11][15]. For example, the CD-variations can be attributed to either mask inaccuracy, proximity effects, lens aberrations, or combinations thereof. In this paper, we do not deal with the real physical origin of these variations. Instead, we capture them in terms of the "true geometrical variations" which we assume to be statistically independent. Examples of such variations are CD variations, ILD thickness variations, or metal layer thickness variations.

Manufacturing variations are random in nature, and generally classified into two categories: temporal and spatial. Temporal variations are due to time-varying equipment conditions, incoming wafer or consumable material characteristics. They manifest themselves as *lot-to-lot* or *wafer-to-wafer* variations. On the other hand, spatial variations can occur on the wafer-to-wafer scale (e.g., due to nonuniformity in the deposition or etch chamber), within-wafer (die-to-die) or within-die[1][16]. We further classify these variations into two categories: global variations and local variations(Fig. 1). Global variations manifest themselves at the wafer-scale, and can be assumed to be constant within specific die. Local

† This work was supported, in part, by the Semiconductor Research Corporation under Contract DC-068.067 and STMicroelectronics.

DAC 99, New Orleans, Louisiana

variations occur at a smaller geometric scale and are more complicated to analyze. For example, if the CD-variations in metal layer are caused by the non-uniform distributions of the exposure dose, then they can be considered as global variations[11]. In contrast, the ILD variations caused by the chemical mechanical polishing (CMP) process depend on the density of the underlying poly-layer, hence they are more suitably treated as local variations[15]. Although local variations can be taken into account due to their systematic nature, in this paper we focus only on global variations and leave the analysis of local variations to future research.

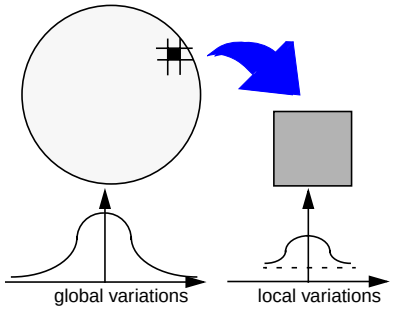

FIGURE 1: Global variations vs. local variations.

It is assumed that the variations in the metal layers are independent from the variations in the active devices. We further assume that the true geometrical variations are mutually independent. For example, we assume not only that the variation of M4 thickness is independent of the variations of M5 thickness, but also that it is independent of the M4 linewidth variation. We believe that this is a valid assumption given the planarization of the subsequent layers in the state-of-the-art IC manufacturing.

Finally, we only consider the first-order effect of the geometric variations on the circuit parameters, i.e., resistance, capacitance and inductance. For instance, if there is a w_1 variation in the M3 width and a w_2 variation in the M3 height, then for a specific segment on this layer, we assume the resistance of that segment can be expressed as:

$$R(w_1,w_2) = R_0 + \Delta R_1 \cdot w_1 + \Delta R_2 \cdot w_2 \quad (1)$$

We normalize the values of ΔR_1 and ΔR_2 so that the values of w_1 and w_2 are between -1 and 1. Similarly, for any capacitance in the circuit subject to the variations w_1 and w_2 we can express the variational value of the capacitance as:

$$C(w_1,w_2) = C_0 + \Delta C_1 \cdot w_1 + \Delta C_2 \cdot w_2 \quad (2)$$

Although there is no restriction on the number of variations in our approach, for notational simplicity we consider only these two variation sources throughout this paper.

2.2. Reduced-order model with variations

Any linear RLC circuit can be described by its MNA equations:

$$(G + sC)x = b \quad (3)$$

When resistance and capacitance parameters are subject to variations of the form in (1) and (2), the MNA terms in the G and C matrices are also subject to the same variations:

$$\begin{aligned} G(w_1, w_2) &= G_0 + \Delta G_1 w_1 + \Delta G_2 w_2 \\ C(w_1, w_2) &= C_0 + \Delta C_1 w_1 + \Delta C_2 w_2 \end{aligned} \quad (4)$$

Combine (4) with (3):

$$(G(w_1, w_2) + sC(w_1, w_2))x = b \quad (5)$$

Equation (5) is essentially a set of ordinary-differential equations with varying parameters. It is seemingly impossible to analyze the effect of variations w_1 and w_2 without directly referring to the full description in (5). However, as we will show in the remaining portions of the paper, when the magnitudes of the variations are reasonably small, key characteristics of the circuit, such as the poles, only "fluctuate" in the proximity of the poles of the nominal circuit. This enables us to construct a compact model of (5) with direct inclusion of variations w_1 and w_2. This compact model is more efficient than the full description. More importantly, without the unnecessary details in the full description, the compact model will provide a better understanding of the variational effects on key circuit characteristics.

2.3. Projection-based model order-reduction

Model order-reduction generates a compact analytic admittance/impedance model by matching *moments*[10] or *poles*[8]. In order to overcome the instability caused by numerical noise for high orders of approximation, projection-based order reduction via the Lanczos or Arnoldi algorithm can be used as part of the moment or pole matching process[4].

In this paper we consider two projection-based order-reduction techniques, PACT[8] and PRIMA[9]. However, our approach can also be extended to other model order-reduction methods such as MPVL[3] and the Arnoldi method in [13]. Due to limited space we will only discuss the PACT-based method in detail, since it most clearly demonstrates our variational approach. It should be noted that our description of PACT is slightly different from the original version in [8].

2.3.1. PACT

An RC circuit is uniquely described by a conductance matrix G and a susceptance matrix C, as shown in (3). In PACT, these two matrices are further partitioned as:

$$G = \begin{bmatrix} G_P & G_C^T \\ G_C & G_I \end{bmatrix}, \quad C = \begin{bmatrix} C_P & C_C^T \\ C_C & C_I \end{bmatrix} \quad (6)$$

where G_P is the port conductance matrix, G_I is the internal conductance matrix and G_C is the connection matrix. The susceptance matrix C is partitioned in the same way. G^T denotes the transpose operation of matrix G. If we denote x_P as a port voltage vector, x_I as an internal voltage vector, and b_P as a port excitation vector, then the circuit can be expressed as:

$$\left(\begin{bmatrix} G_P & G_C^T \\ G_C & G_I \end{bmatrix} + s \begin{bmatrix} C_P & C_C^T \\ C_C & C_I \end{bmatrix} \right) \begin{bmatrix} x_P \\ x_I \end{bmatrix} = \begin{bmatrix} b_P \\ 0 \end{bmatrix} \quad (7)$$

It can be shown that G_P, G_I, C_P and C_I are symmetric[8]. For a circuit with a unique dc solution it also can be shown that G_I is positive semi-definite. Note that for most interconnect analysis problems, the size of G_P is small while the size of G_I is large. The admittance matrix, which has a size equal to the number of ports, can be obtained from (7):

$$Y(s) = G_P + sC_P - (G_C + sC_C)^T \cdot (G_I + sC_I)^{-1} \cdot (G_C + sC_C) \quad (8)$$

The PACT algorithm consists of two congruence transformations, TC-1 and TC-2. TC-1 is the same as matching the first moment m_0 in the moment-matching approaches such as

AWE[10], thereby preserving the dc gain of the reduced-order model. It is performed by applying a congruence transformation X on both G and C, where X is defined as:

$$X = \begin{bmatrix} I & 0 \\ -G_I^{-1}G_C & I \end{bmatrix} = \begin{bmatrix} I & 0 \\ V & I \end{bmatrix} \quad (9)$$

The resulting new conductance and susceptance matrices are:

$$G' = X^T G X = \begin{bmatrix} G_P + G_C^T V & 0 \\ 0 & G_I \end{bmatrix} = \begin{bmatrix} G'_P & 0 \\ 0 & G_I \end{bmatrix} \quad (10)$$

and

$$C' = \begin{bmatrix} C_P + V^T C_C + C_C^T V + V^T C_I V & (C_C + C_I V)^T \\ C_C + C_I V & C_I \end{bmatrix} = \begin{bmatrix} C'_P & C'^T_C \\ C'_C & C_I \end{bmatrix} \quad (11)$$

It can be shown that after TC-1, the admittance matrix is:

$$Y(s) = G'_P + sC'_P - s^2 C'^T_C (G_I + sC_I)^{-1} C'_C \quad (12)$$

TC-2 then generates a compact model by dropping the non-dominant poles. Here we express it in the context of a *generalized eigenvalue problem*, which is based on the following theorem[14]:

Theorem 1: *For symmetric matrix pair (A, B), let B be positive definite. Then there exist a nonsingular matrix U satisfying $U^TBU=I$ such that $U^TAU=\Lambda$, where Λ is real and diagonal.*

Following Theorem 1, (12) can be re-written as:

$$Y(s) = G'_P + sC'_P - s^2 C'^T_C U^T (I + s\Lambda)^{-1} U C'_C \quad (13)$$

Note that in (13) matrix U is still a square matrix and its column space is a complete set of generalized eigenvectors of the symmetric pair (G_I, C_I). If we choose only a few eigenvectors corresponding to the dominant eigenvalues, then a reduced-order model can be generated:

$$Y_r(s) = G'_P + sC'_P - s^2 C'^T_C U_r^T (I + s\Lambda_r)^{-1} U_r C'_C \quad (14)$$

There are many methods to calculate the dominant eigenvector matrix U_r without the complete factorization of matrix pair (G_I, C_I). The most efficient method is applying Cholesky factorization and Lanczos methods[4]. Because G_I is positive semi-definite, a Cholesky factorization can be applied as:

$$G_I = LL^T \quad (15)$$

Thus part of (12) can be written as:

$$(G_I + sC_I)^{-1} = (LL^T + sC_I)^{-1} = L^{-T}(I + sL^{-1}C_I L^{-T})^{-1} L^{-1}$$
$$= L^{-T}(I + sX\Lambda X^T)^{-1} L^{-1} = L^{-T} X (I + s\Lambda)^{-1} X^T L^{-1}$$

where column space of X are the eigenvectors of $L^{-1}C_IL^{-T}$. If only the dominant eigenvectors are calculated using Lanczos algorithm and are grouped into X_r, then:

$$U_r = X_r^T L^{-1} \quad (16)$$

Because G_I is a sparse matrix, its Cholesky factorization L is also sparse. Thus, the inversion of L is easy to calculate. It is trivial to show that the above procedure is essentially identical to the original PACT technique. When relatively high orders of approximation are required, an improved Lanczos algorithm such as LASO is required[4]. However, such cases are generally RLC circuits for which we use PRIMA.

2.3.2. PRIMA

In PRIMA, an RLC circuit is described by four matrices (G, C, B, L), which are defined by:

$$\begin{cases} C \cdot \dfrac{dx}{dt} + G \cdot x = B \cdot u_p \\ i_p = L^T \cdot x \end{cases} \quad (17)$$

Note that matrices G and C are constructed in a different way than PACT. The key problem in PRIMA is to calculate an invariant subspace X, or *Krylov subspace*, of matrix $A \equiv -G^{-1}C$, such that:

$$X^T X = I_q, \qquad X^T A X = H_q \quad (18)$$

Where H_q is a block Hessenberg matrix. Note that the rank of X is much smaller than the rank of the original matrix A. A reduced-order model, $(\tilde{G}, \tilde{C}, \tilde{B}, \tilde{L})$, can be generated by projecting the original system onto this invariant subspace:

$$\tilde{G} = X^T G X, \quad \tilde{C} = X^T C X$$
$$\tilde{B} = X^T B, \quad \tilde{L} = X^T L \quad (19)$$

3. VARIATIONAL ANALYSIS

3.1. Results in matrix perturbation theory

The key problem in our variational analysis is to find the relationship between the variations and the dominant eigenvalues/eigenvectors. Fortunately, the matrix perturbation theory gives us some insight into the variational behavior of the eigenvalues/eigenvectors, as summarized in the following theorems[6][14].

Theorem 2: *Let A be a symmetric matrix with eigenvalues:*

$$\lambda_1 \geq \lambda_2 \geq \ldots \geq \lambda_n \quad (20)$$

and $\tilde{A} = A + E$ *denote a symmetric perturbation of A with eigenvalues:*

$$\tilde{\lambda}_1 \geq \tilde{\lambda}_2 \geq \ldots \geq \tilde{\lambda}_n \quad (21)$$

Let the eigenvalues of E be:

$$\varepsilon_1 \geq \varepsilon_2 \geq \ldots \geq \varepsilon_n \quad (22)$$

Then, for $i = 1, \ldots, n$,

$$\tilde{\lambda}_i \in [\lambda_i + \varepsilon_n, \lambda_i + \varepsilon_1] \quad (23)$$

In our application, the magnitude of the perturbation, matrix E, is generally small. Thus the above theorem guarantees the variational eigenvalues be in the proximity of the nominal eigenvalues. The next theorem describes the behavior of the variational eigenvectors:

Theorem 3: *For a symmetric matrix pair (A,B), let B be positive definite. For matrices X_1 and X_2 such that*

$$\begin{bmatrix} X_1^T \\ X_2^T \end{bmatrix} A \begin{bmatrix} X_1 & X_2 \end{bmatrix} = \begin{bmatrix} A_1 & 0 \\ 0 & A_2 \end{bmatrix}, \quad \textbf{and} \quad \begin{bmatrix} X_1^T \\ X_2^T \end{bmatrix} B \begin{bmatrix} X_1 & X_2 \end{bmatrix} = \begin{bmatrix} B_1 & 0 \\ 0 & B_2 \end{bmatrix}$$

where

$$A_1 = \mathrm{diag}(\alpha_1, \ldots, \alpha_k), \quad A_2 = \mathrm{diag}(\alpha_{k+1}, \ldots, \alpha_n)$$
$$B_1 = \mathrm{diag}(\beta_1, \ldots, \beta_k), \quad B_2 = \mathrm{diag}(\beta_{k+1}, \ldots, \beta_n) \quad (24)$$

Given symmetric perturbations of E and F such that:

$$\tilde{A} = A + E, \quad \tilde{B} = B + F$$

If the distance between the eigenvalue clusters of (A_1, B_1) and (A_2, B_2) is sufficiently large, and the perturbations E and F are sufficiently small, then there exist matrices P and Q such that the columns of

$$\tilde{X}_1 = X_1 + X_2 P, \quad \tilde{X}_2 = X_2 + X_1 Q^T \tag{25}$$

span the eigenspace of pair $(\tilde{A}, \tilde{B})$.

3.2. Variational analysis of PACT

3.2.1. Variational analysis of TC-2

Theorem 3 is very attractive in the context of PACT algorithm. If we regard X_1 as the dominant eigenvectors of the matrix pair (G_I, C_I) from (6), then the theorem actually tells us how the dominant eigenvectors behave under the influence of the variations. However, direct application of Theorem 3 is not practical because matrices P and Q can only be calculated after solving a set of *generalized Sylvester equations*. Furthermore, even if we know the matrix P, we still have to calculate the non-dominant eigenvectors X_2. The consequence is that we have to perform a complete eigen-decomposition of the matrix pair (G_I, C_I). The complete eigen-decomposition is very costly and is actually in the opposite objective of order-reduction.

Intuitively, we can see that the values of P and Q in Theorem 3 depend on the perturbations E and F. When there is no perturbation, P will be identically zero. Because the magnitudes of the variations are small, a Taylor expansion can be used to express the variational eigenvalues and eigenvectors, but the Taylor expansion is of a higher dimension. This principle has been used in quantum mechanics for decades[7], and the parameters of the Taylor expansion can be calculated by solving a set of linear equations.

More specifically, assume that Λ_r and U_r are the dominant eigenvalues/eigenvectors of the matrix pair (G_I, C_I). If the internal conductance matrix and internal susceptance matrix are subject to the following variations:

$$\begin{aligned} G_I(w_1, w_2) &= G_{I0} + \Delta G_{I1} w_1 + \Delta G_{I2} w_2 \\ C_I(w_1, w_2) &= C_{I0} + \Delta C_{I1} w_1 + \Delta C_{I2} w_2 \end{aligned} \tag{26}$$

then Λ_r and U_r are in the format of:

$$\begin{aligned} \Lambda_r &= \Lambda_{r0} + \Delta\Lambda_{11} w_1 + \Delta\Lambda_{12} w_1^2 + \Delta\Lambda_{21} w_2 + \Delta\Lambda_{22} w_2^2 \\ U_r &= U_{r0} + \Delta U_{11} w_1 + \Delta U_{12} w_1^2 + \Delta U_{21} w_2 + \Delta U_{22} w_2^2 \end{aligned} \tag{27}$$

In order to determine the parameters involved in (27), we pick up some "sample points" and calculate the dominant eigenvalues/ eigenvectors. The parameters are uniquely determined by a set of linear equations. Here we choose sample point as ($w_1 = 0$, $w_2 = 0$), (1,0), (-1,0), (0,1) and (0,-1).

3.2.2. Variational analysis of TC-1

Recall that the purpose of the first congruence transformation, TC-1, is to preserve the dc gain. The key point in TC-1 is calculating $V = -G_I^{-1} G_C$. When G_I and G_C are subject to variations, we expect V to depend on the variations as well. By a careful review of the KCL description in (7), we find that V can actually be calculated by obtaining the dc solution of the circuit. In (7), if we assume the susceptance matrix is identically zero and there is no current injection to all internal nodes, then the port and internal voltages can be expressed as:

$$G_C x_p + G_I x_I = 0 \tag{28}$$

from which:

$$x_I = -G_I^{-1} G_C x_P = V x_P \tag{29}$$

Thus, if we drive one port node with a unit voltage source and ground all the remaining port nodes, then the dc solution of all the internal nodes will be the corresponding column of the matrix V. Repeating this procedure will generate the complete matrix. Note that in this process, only the excitation vector of the MNA formulation needs to be modified. Thus only one LU factorization is need in the whole process.

If we assume that the variational matrix V can be expressed as:

$$V(w_1, w_2) = V_0 + \Delta V_1 w_1 + \Delta V_2 w_2 \tag{30}$$

then parameters ΔV_1 and ΔV_2 are actually sensitivities of the internal node voltages. We can then use adjoint sensitivity analysis[2] to calculate these sensitivities. Note that in the adjoint sensitivity analysis, no extra LU factorization is needed. Instead, the sensitivities are calculated by multiple backward- and forward-substitutions.

However, because sensitivities are only accurate within a very small range close to the nominal values, in practice we found that the results obtained by adjoint sensitivity are not satisfactory. To improve the accuracy, we once again use the perturbation expansion to express the variational V as:

$$V(w_1, w_2) = V_0 + \Delta V_{11} w_1 + \Delta V_{21} w_2^2 + \Delta V_{12} w_2 + \Delta V_{22} w_2^2 \tag{31}$$

The parameters are calculated in the same manner as those in TC-2.

3.2.3. Overall flow of variational analysis in PACT

To summarize, we assume that the variations of the conductance matrix and susceptance matrix can be expressed as:

$$\begin{aligned} G(w_1, w_2) &= G_0 + \Delta G_1 w_1 + \Delta G_2 w_2 \\ C(w_1, w_2) &= C_0 + \Delta C_1 w_1 + \Delta C_2 w_2 \end{aligned} \tag{32}$$

If we partition the two matrices in a manner similar to that in (6), then we have the following:

$$\begin{aligned} G_P(w_1, w_1) &= G_{P0} + \Delta G_{P1} w_1 + \Delta G_{P2} w_2 \\ G_I(w_1, w_2) &= G_{I0} + \Delta G_{I1} w_1 + \Delta G_{I2} w_2 \\ G_C(w_1, w_2) &= G_{C0} + \Delta G_{C1} w_1 + \Delta G_{C2} w_2 \\ C_P(w_1, w_2) &= C_{P0} + \Delta C_{P1} w_1 + \Delta C_{P2} w_2 \\ C_I(w_1, w_2) &= C_{I0} + \Delta C_{I1} w_1 + \Delta C_{I2} w_2 \\ C_C(w_1, w_2) &= C_{C0} + \Delta C_{C1} w_1 + \Delta C_{C2} w_2 \end{aligned} \tag{33}$$

There are two variational congruence transformations, denoted VTC-1 and VTC-2, similar to the two congruence transformations in PACT.

- VTC-1

Calculate ΔV_{11}, ΔV_{12}, ΔV_{21}, ΔV_{22} in (31) by Taylor expansion. In the results of VTC-1, all the terms with order higher than 2 are dropped. Thus:

$$\begin{aligned} G'_P(w_1, w_2) &= G'_{P0} + \Delta G'_{P11} w_1 + \Delta G'_{P12} w_1^2 + \Delta G'_{P21} w_2 + \Delta G'_{P22} w_2^2 \\ C'_P(w_1, w_2) &= C'_{P0} + \Delta C'_{P11} w_1 + \Delta C'_{P12} w_1^2 + \Delta G'_{P21} w_2 + \Delta G'_{P22} w_2^2 \\ C'_C(w_1, w_2) &= C'_{C0} + \Delta C'_{C11} w_1 + \Delta C'_{C12} w_1^2 + \Delta C'_{P21} w_2 + \Delta C'_{P22} w_2^2 \end{aligned}$$

where

$$\begin{aligned} G'_{P0} &= G_{P0} + G_{C0}^T V_0 \\ \Delta G'_{P11} &= \Delta G_{P1} + \Delta G_{C1}^T \cdot V_0 + G_{C0}^T \cdot \Delta V_{11} \\ \Delta G'_{P12} &= \Delta G_{C1}^T \cdot \Delta V_{11} + G_{C0}^T \cdot \Delta V_{12} \end{aligned} \tag{34}$$

and

$$C'_{C0} = C_{C0} + C_{I0}V_0$$
$$\Delta C'_{C11} = C_{C1} + C_{I0} \cdot \Delta V_{11} + \Delta C_{I1} \cdot V_0 \quad (35)$$
$$\Delta C'_{C12} = \Delta C_{I1} \cdot \Delta V_{11} + C_{I0} \cdot \Delta V_{12}$$

Furthermore

$$C'_{P0} = C_{P0} + V_0^T C_{C0} + C_{C0}^T V_0 + V_0^T C_{I0} V_0$$
$$\Delta C'_{P11} = \Delta C_{P1} + \Delta V_{11}^T \cdot C_{C0} + V_0^T \cdot \Delta C_{C1} + \Delta C_{C1}^T \cdot V_0 + $$
$$+ C_{C0}^T \cdot \Delta V_{11} + V_0^T C_{I0} \Delta V_{11} + V_0^T \Delta C_{I1} V_0 + \Delta V_{11}^T C_{I0} V_0$$
$$\Delta C'_{P12} = \Delta V_{11}^T \Delta C_{C1} + \Delta C_{C1}^T \Delta V_{11} + V_0^T \Delta C_{I1} \Delta V_{11} + $$
$$+ \Delta V_{11}^T C_{I0} \Delta V_{11} + \Delta V_{11}^T \Delta C_{I1} V_0 + \Delta V_{12}^T C_{C0} + $$
$$+ C_{C0}^T \Delta V_{12} + \Delta V_{12}^T C_{I0} V_0 + V_0^T C_{I0} \Delta V_{12}$$

All the terms related to w_2 can be handled similarly.

- VTC-2

For the variational pair, $(G_I(w_1, w_2), C_I(w_1, w_2))$ we use the expansion method discussed in the previous subsection to calculate the expansion parameters:

$$\Lambda_r(w_1, w_2) = \Lambda_{r0} + \Delta\Lambda_{r11} w_1 + \Delta\Lambda_{r12} w_1^2 + \Delta\Lambda_{r21} w_2 + \Delta\Lambda_{r22} w_2^2$$
$$U_r(w_1, w_2) = U_{r0} + \Delta U_{r11} w_1 + \Delta U_{r12} w_1^2 + \Delta U_{r21} w_2 + \Delta U_{r22} w_2^2$$

The variational reduced-order model is then given by:

$$Y_r(s) = G'_P(w_1, w_2) + sC'_P(w_1, w_2) - $$
$$- s^2 C''^T_C(w_1, w_2)(I + s\Lambda_r(w_1, w_2))^{-1} C''_C(w_1, w_2) \quad (36)$$

with term $C''_C(w_1, w_2)$ expressed as:

$$C''_C(w_1, w_2) = C''_{C0} + \Delta C''_{C11} w + \Delta C''_{C12} w_1^2 + $$
$$+ \Delta C''_{C21} w_2 + \Delta C''_{C22} w_2^2 \quad (37)$$

where

$$C''_{C0} = U_{r0} C'_{C0}$$
$$\Delta C''_{C11} = \Delta U_{r11} C'_{C0} + U_{r0} \Delta C'_{C11} \quad (38)$$
$$\Delta C''_{C12} = U_{r0} \Delta C'_{C12} + \Delta U_{r11} \Delta C'_{C11} + \Delta U_{r12} C'_{C0}$$

The parameters related to w_2 can be calculated in a similar way.

3.3. Variational analysis of PRIMA

The key objective of PRIMA is to calculate an invariant subspace which forms the column space of matrix X. Therefore, we apply the following theorem regarding invariant subspace[14].

Theorem 4: *Let $(X_1\ Y_2)$ be unitary and suppose that column space of X_1 is a simple invariant subspace of A, so that*

$$\begin{bmatrix} X_1^T \\ Y_2^T \end{bmatrix} A \begin{bmatrix} X_1 & Y_2 \end{bmatrix} = \begin{bmatrix} L_1 & H \\ 0 & L_2 \end{bmatrix} \quad (39)$$

Given a perturbation E, if the spectra of L_1 and L_2 are sufficiently far away and the perturbation is sufficiently small, then there exists a matrix P, such that

$$\tilde{X}_1 = (X_1 + Y_2 P)(I + P^T P)^{-1/2}$$
$$\tilde{Y}_2 = (Y_2 - X_1 P^T)(I + PP^T)^{-1/2} \quad (40)$$

form the orthonormal bases for simple right and left invariant subspace of $A + E$.

Once again, it is impractical to calculate matrix P. Instead, we seek to calculate the expansion of the Krylov subspace:

$$X(w) = X_0 + \Delta X_1 w + \Delta X_2 w^2 \quad (41)$$

The parameters are also calculated by choosing sample points. A variational reduced-order can then be constructed by inserting the resulting variational Krylov-subspace into (19) and collecting variational terms up to the 2nd-order.

4. EXAMPLES

Both the PACT-based and PRIMA-based variational analysis algorithms have been implemented in C as SPICE-in-SPICE-out analysis tools.

4.1. Top-level of a clock tree

The first example is the top-level of the clock tree in a 0.35μ industrial design. This level carries the clock signal from the center of the block to seven distinct locations in the block, from which the signal is distributed to the second-level. The top-level is routed solely in metal layers M2, M3 and M4. The widths of these three layers are subject to 3σ-variations with magnitude of up to 30%. The circuit is modeled as an 8-port and the order of the approximation is 5. Variational analysis was performed on the 8-port.

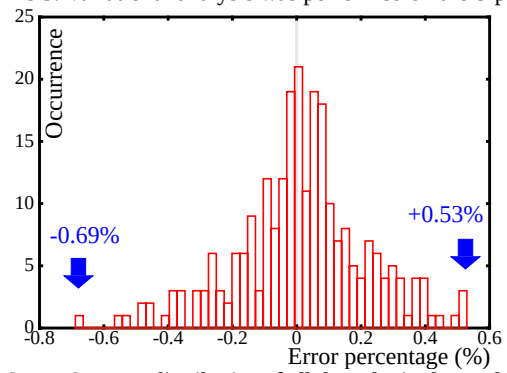

FIGURE 2: Error distribution of all the poles in the top-level clock tree example.

In order to demonstrate the accuracy of our variational reduced-order model, we performed 50 tests. In each test, a set of three uniformly distributed numbers is generated as the width variations of the three metal layers. The original netlist is modified based on these variations and a reduced-order model is directly calculated as the true value. The second reduced-order model is generated by using the variational reduced-order model. We then compared the difference between the poles and residues of these two reduced-order models. The distribution of error in the poles is shown in Fig. 2. For the figure, 77% of the tests have the error between -0.2% and +0.2%, even though the poles varied by as much as 27%.

We further perform multiple SPICE simulations for models constructed in two different methods under multiple variations. The results of the first 10 test are tabulated in Table 1.

TABLE 1: Fifty-percent delay at a fan-out node in Example 1.

Variations (30% 3σ)			Fan-out Delay (ps)	
M2-w	M3-w	M4-w	Direct	Variational
-17.25%	+20.35%	+7.73%	388.49	388.72
-2.91%	-27.37%	-28.37%	334.45	334.81
-17.25%	+20.35%	+7.73%	388.49	388.72
+20.77%	+1.51%	-17.84%	357.99	357.88
+2.04%	+13.63%	-11.44%	368.74	368.66

TABLE 1: Fifty-percent delay at a fan-out node in Example 1.

Variations (30% 3σ)			Fan-out Delay (ps)	
M2-w	M3-w	M4-w	Direct	Variational
+13.65%	+29.97%	+29.97%	413.82	414.58
+13.65%	-1.30%	+3.29%	377.29	377.31
-5.28%	+14.67%	-13.92%	366.40	366.28
+10.93%	-11.83%	+2.50%	372.11	371.97
-26.55%	-7.95%	+7.89%	377.11	377.02

4.2. Three closely coupled nets

The second example is extracted from a 0.25μ industrial design. The circuit consists of three closely-coupled nets routed on layers Metal 4 and Metal 5. The process is characterized by ±20% variations in linewidth and height for both M4 and M5 metal layers (3σ). We once again constructed the reduced-order model with the inclusion of those variations. We performed 50 SPICE simulations with randomly generated variations to test the accuracy of our model. The results of the first 10 are listed in Table 2.

TABLE 2: Fifty-percent delay at a fan-out node in Example 2.

Variations (20% 3σ)				Fanout delay(ps)	
M4-w	M4-h	M5-w	M5-h	Direct	Vari.
-16.67%	-13.05%	-8.41%	-4.20%	2114.5	2115.7
+15.21%	-5.12%	-10.64%	-4.29%	2288.6	2288.5
+16.04%	+5.99%	+11.13%	+15.90%	2463.7	2464.2
+12.67%	+17.47%	+0.93%	-2.07%	2431.0	2431.1
+6.36%	+10.27%	-5.60%	-1.11%	2374.0	2374.2
+14.42%	-4.03%	-13.58%	-13.02%	2245.5	2245.1
-15.18%	+9.97%	-13.54%	-18.51%	2223.7	2225.1
+11.65%	+0.76%	-6.44%	-14.82%	2272.4	2272.3
-19.36%	-6.84%	-19.47%	-18.38%	2044.5	2046.0
+1.37%	-13.40%	-14.03%	-2.70%	2180.9	2181.2

4.3. A simple RLC circuit

To demonstrate the variational analysis of PRIMA, we constructed a three-segment RLC circuit. The capacitance of each segment is 2pF and the inductance 1nH. The resistance of each segment is 10Ω, 2Ω and 35Ω, respectively. Segments 1 and 3 were subjected to a common variation of up to 15% in magnitude for the R, L and C values. A variational reduced-order model was constructed. The Bode plots for an admittance with of 13.5% are shown in Fig. 3. As we can see, the variational analysis matches the directly calculated reduced-order extremely well.

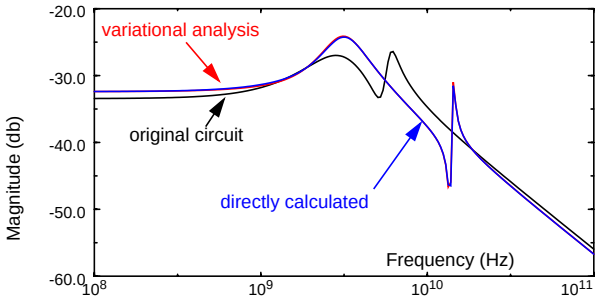

FIGURE 3: Bode plot of an admittance term in RLC example with variation of +13.5%. Note that directly calculated and variational model results are overlapping.

5. CONCLUSION

In this paper we present a novel order-reduction technique for variational analysis of the RLC interconnect circuits. The technique constructs a reduced-order model with the direct inclusion of the statistically independent geometrical variations. Experiments on industrial examples demonstrate the satisfactory accuracy for multiple variations with magnitudes up to 30% which cover the typical 3σ ranges in the DSM technologies.

REFERENCES

[1]Boning, D.S. and J.E. Chung, "Statistical metrology-measurement and modeling of variation for advanced process development and design rule generation", *Proc. 1998 Int. Conf. on Characterization and Metrology for ULSI Technology*, March 1998.

[2]Director, S.W. and R.A. Rohrer, "The generalized ajoint network and network sensitivities", *IEEE Tran. Circuit Theory*, vol. CT-16, No. 3, August 1969.

[3]Feldmann, P. and R.W. Fruend, "Efficient linear circuit analysis by Padé approximation via the Lanczos process", *IEEE Trans. CAD*, vol. 14, May 1995.

[4]Golub, G.H. and C.F. Van Loan, *Matrix computations*, 3rd ed., The Johns Hopkins University Press, Baltimore 1996.

[5]Harkness, C.L. and D.P. Lopresti, "Interval methods for modeling uncertainty in RC timing analysis", *IEEE Trans. CAD*, vol. 11, No. 11, November 1992.

[6]Kato, T., *Perturbation theory for linear operator*, 2nd ed., Springer-Verlag, 1995.

[7]Kemble, E.C., *The fundamental principles of quantum mechanics*, Dover, 1958.

[8]Kerns, K.J. and A.T. Yang, "Stable and efficient reduction of large, multiport RC networks by pole analysis via congruence transformations", *IEEE Trans. CAD*, vol. 16, 1997.

[9]Odabasioglu, A., M. Celik and L.T. Pileggi, "PRIMA: passive reduced-order interconnect macromodeling algorithm", *IEEE Trans. CAD*, August 1998.

[10]Pillage, L.T. and R.A. Rohrer, "Asymptotic waveform evaluation for timing analysis", *IEEE Trans. CAD*, vol. 9, April 1990.

[11]Progler, C., H. Du and G. Wells, "Potential causes of across field CD variation", *SPIE*, vol. 3051, 1997.

[12]Rubinstein, J., P. Penfield Jr. and M.A. Horowitz, "Signal delay in RC tree networks", *IEEE Trans. CAD*, vol. CAD-2, July 1983.

[13]Silveira, L.M., M. Kamon and J. White, "Efficient reduced-order modeling of frequency-dependent coupling inductances associated with 3-D interconnect structures", *Proc. 32nd ACM/IEEE Design Automation Conference*, June 1995.

[14]Stewart, G.W. and J.-G. Sun, *Matrix perturbation theory*, Academic Press, Inc., San Diego, 1990

[15]Stine, B.E. *et al*, "The physical and electrical effects of metal filling patterning practices for oxide chemical mechanical polishing processes", *IEEE Trans. Electron Devices*, vol. 45, No. 3, March 1998.

[16]Stine, B.E. *et al*, "Rapid characterization and modeling of spatial variation: a CMP case study", *CMP Metrology Session*, Semicon West '97, July 1997.